

Stereoselectivity in the Diels–Alder addition of S-hydroxy-N-methylsuccinimide acrylate to cyclopentadiene: origins and DFT computational models

S. M. Bakalova, J. Kaneti

Institute of Organic Chemistry with Centre of Phytochemistry, Bulgarian Academy of Sciences, Acad. G. Bonchev street, bl. 9, 1113 Sofia, Bulgaria

Received March 02, 2017; Revised March 24, 2017

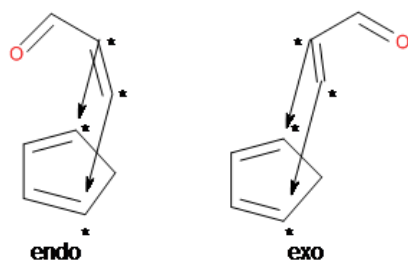
Dedicated to Acad. Bogdan Kurtev on the occasion of his 100th birth anniversary

The title Diels–Alder reaction is used as computational test example of the performance of several DFT functionals at various levels of parameterization. We show that experimental diastereoface selectivities, kinetically corresponding to free activation energy differences of the order of less than 1 kcal.mol⁻¹, can be successfully reproduced by computations using most recent extensively parameterized functionals as M06L, M06-2x and MN12sx, while taking into account the conformational distribution of reactants, in the present case S-hydroxy-N-methylsuccinimide acrylate. Presently computed important contributions to intermolecular interactions between acrylate and cyclopentadiene, governed by dienophile conformation, cannot be assigned only to electrostatic origins in the cases of diastereoface selectivity. In the broader case of *endo:exo* selectivity, contributions of dispersion and longer range repulsion have also been accounted for.

Key words: Diels–Alder stereoselectivity; reactant conformations; transition structures; activation free energies; DFT calculations

INTRODUCTION

The cycloaddition of olefins to dienes, discovered by Diels and Alder in the 1920-ies [1, 2] is still among the most important reactions in organic synthesis. This unabating interest is due to its unique capability to generate up to four chiral centres in a single reaction step, Scheme 1.



Scheme 1. Steric aspects of the [2+4] addition of acrylate to cyclopentadiene. The four prochiral carbon atoms, evolving to chiral centres in the course of DA reaction, are denoted by asterisks.

The latter fact substantiates the continuing effort to elucidate the electronic and steric aspects of its mechanism, reaction rate and stereoselectivity. The development of insights into the Diels–Alder, DA,

mechanism as a [4+2] electrocyclic addition, started with the works of R. Woodward and R. Hoffmann [3], is still based on their ideas and terminology of orbital symmetry.

Interpretations of DA diastereoselectivity are concerned mainly with the *endo vs. exo* selectivity, Scheme 1, with the former usually dominating the reaction outcome [4, 5]. Recent decades of computational studies have witnessed a widening use of density functional theory, DFT [6], treatments of this type of selectivity. However, serious deficiencies in the theoretical predictions have also been revealed [7, 8]. Correct, while still sufficiently robust, computational predictions related to DA stereoselectivity only became possible with recent extensive parameterizations of DFT functionals [8–11]. Thus, the use of DFT computations in the interpretation of DA *endo vs. exo* selectivity is nowadays reliable and theoretically substantiated. The second type of DA selectivity, related to the directionality of the dienophile approach to the planar diastereotopic faces of the diene, is usually modelled by DFT calculations qualitatively correctly. Another computational alternative, namely the use of wavefunction (or MO) theory [12], has also been shown to correctly reproduce the two types of Diels–Alder reaction selectivity using explicit treatment of dynamic electron correlation [8], and

* To whom all correspondence should be sent:

E-mail: bakalova@orgchm.bas.bg;

kaneti@orgchm.bas.bg

can be used as reference, even though at a significantly higher computational cost.

EXPERIMENTAL

Computational details

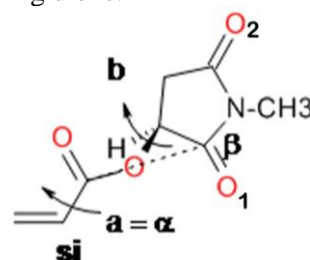
DFT modeling of the reaction is carried out using the GAUSSIAN 09 suite of programs [13]. Several functionals are used in the DFT calculations: PBE0 [14, 15], B97D [16], M06L, M06-2x [9–11]. We also use the recent precisely parameterized Minnesota functionals: M11L [17, 18] and MN12sx [19]. Transition structures, TSs, on the studied diastereoisomeric reaction paths are located using standard optimization techniques and are verified via vibrational analysis to possess a single imaginary frequency, as well as by intrinsic reaction coordinate following [20]. Solvent effects are considered using the PCM approximation [21] in dichloromethane, DCM.

RESULTS AND DISCUSSION

Experiments with acryloyl-*S*-hydroxy-*N*-methyl succinimide, AS, Scheme 2, as the dienophile [22] show low *endo:exo* and diastereoface selectivity of the addition to cyclopentadiene, CPD, in dichloromethane, DCM.

Here, we consider the possible reaction products on the basis of the distribution of existing conformational isomers of the dienophile.

As shown in Fig. 1, rotation from the *s-cis* center, to the *s-trans*-isomer, left, of the dienophile changes the upper face of the prochiral fragment from **si** to **re**, while virtually leaving the diene approach face, electrostatically assisted by the adjacent carbonyl group, intact. *Vice versa*, a change in the relative orientation of carbonyl groups and dipoles does not alter the configuration of prochiral faces, but changes the attack preference of the incoming diene.



Scheme 2. Conformational degrees of freedom in the dienophile AS with respect to internal rotations around **a** = α and **b**; α determining *s-cis* – *s-trans* isomerism, while the rotation around the ester bond **b** is chosen to determine the dihedral angle β , or $\text{O}=\text{C}---\text{C}=\text{O}_1$, to define the mutual orientation of the two carbonyl bond dipoles at the acrylate fragment and next to the chiral carbon, connected by a dashed line. Carbonyl bonds prefer either the positive, or the negative perpendicular orientation β to each other. [23, 24] As the $\text{OC}---\text{CO}_1$ dihedral angle is equivalent to rotation around a $\text{Csp}^3 - \text{Csp}^3$ bond, the conformation energy profile should possess 3 minima. DFT conformation analysis favors positive β for both *s-cis*- AS (ASC) and *s-trans*- AS (AST) configurations and also reveals two more minima of slightly higher energy with negative β , Table 1.

Table 1. Total (in hartrees) and relative (in kcal.mol^{-1}) energies of *s-cis*-acryloyl-*S*-hydroxy-*N*-methyl succinimide, ASC, and *s-trans*-acryloyl-*S*-hydroxy-*N*-methyl succinimide, AST, conformers of the dienophile, M062x/6-311G(d,p), DCM.

Str.	E(total)	E + ZPE	E + ΔG_{298}	$\Delta\Delta G$	OCCO_1	OCCO_2
ASC1	-665.866542	-665.696842	-665.736794	0.00	103.3	-47.8
ASC2	-665.864483	-665.695181	-665.735680	0.70	-132.5	57.8
ASC3	-665.864480	-665.695118	-665.735600	0.75	-72.9	118.8
AST1	-665.865717	-665.696064	-665.736326	0.29	103.2	-48.0
AST2	-665.863714	-665.694414	-665.735278	0.95	-73.9	116.9
AST3	-665.863965	-665.694633	-665.735235	0.98	-134.1	56.3

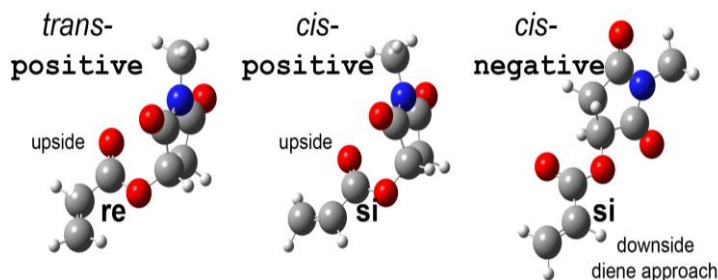
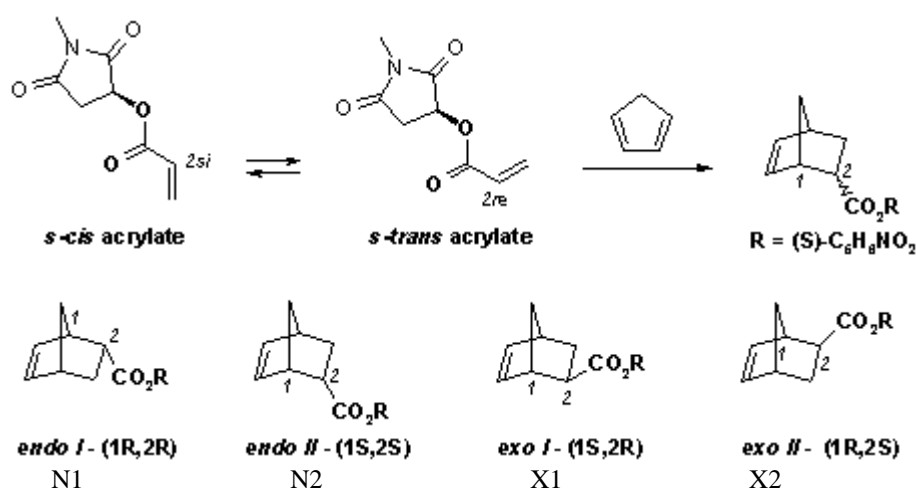


Fig. 1. Conformational effects on prochiral dienophile faces. Configurational designations **re** and **si** refer to the in-plane face. Assuming, for electrostatic reasons, diene approach preference from the side of the adjacent carbonyl group CO_1 , *s-cis* – *s-trans* isomerization directly changes the configuration of the prochiral α -carbon from **re** to **si**, left and center, while positive or negative dihedral angles between acrylate carbonyl and the imide carbonyl group adjacent to the chiral center, center and right, change the preferred direction of attack.

Table 2. Solvent thermodynamics of *s-cis* acryloyl-*S*-hydroxy-*N*-methyl succinimide, ASC, M062x/6-311G++(d,p), along angle β , Scheme 2, $O_{acr} = C \cdots C = O_1$. Stationary point names correspond approximately to the value of β , with TS meaning the respective rotational transition structures.

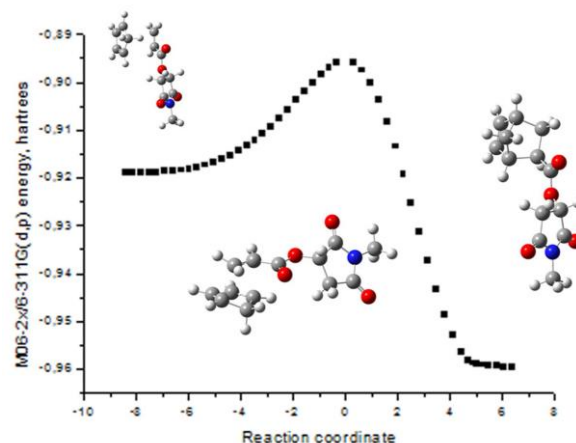
Stationary point	E(total) <i>hartrees</i>	E + ΔG_{298} <i>hartrees</i>	$\Delta\Delta G^\ddagger$ kcal.mol ⁻¹	E + $\Delta G_{(ASC+CPD)}$ <i>hartrees</i>
ASC103	-665.880455	-665.751191	0.00	-859.746234
ASC143TS	-665.867067	-665.737538	8.57	
ASC-133	-665.879063	-665.750244	0.59	-859.745287
ASC-94TS	-665.877827	-665.747966	2.02	
ASC-75	-665.878408	-665.750676	0.32	-859.746540
ASC32TS	-665.866503	-665.736244	9.38	
CPD	-194.061413	-193.995043		

**Scheme 3.** *Endo* and *exo* isomeric products, resulting from the reaction of a single isomer of *S*-hydroxy-*N*-methylsuccinimide acrylate with cyclopentadiene [26, 27]. In transition structures, TSs, acrylate *s-cis* and *s-trans* isomers are possible. In adducts, these isomers cannot be distinguished because of the practically free rotation of the resulting carboxylate group, which is no longer conjugated.

Schemes 1 and 3 outline the origins of four *endo:exo* isomeric product pairs from each of the three conformational isomers of dienophile. Thus, to completely model the reaction in question, we would need to consider computationally 24 diastereoisomeric reaction potential energy paths and obtain the resulting kinetic product distribution from the calculated Gibbs activation free energy differences [25]. However, as the barrier between the two conformers with negative β is less than 2 kcal.mol⁻¹ (Table 2), the corresponding pairs of TSs collapse into each other to give one and only negative- β TS. Thus, the total number of located TS amounts to 16.

Computational results using Pople basis sets, mostly at the 6-311G(d,p) level [28, 29], are listed in Tables 1S and 3. Some of the energetically preferred transition structures are shown in Fig. 3, and the complete product distribution is in Table 3. A general reaction energy profile, *i.e.* the intrinsic reaction coordinate (IRC) for a diastereoisomeric

reaction channel, is shown in Fig. 2: reactants left; product right, separated by a single TS, centre.

**Fig. 2.** A complete electronic energy profile: IRC starting from the TS of the DA addition of CPD to *s-cis* acryloyl-*S*-hydroxy-*N*-methyl succinimide, ASC, M06-2x/6-311G(d,p).

As indicated by computed Gibbs free energies of the 16 diastereoisomeric TSs, there is no single

lowest structure to dominate the stereochemical outcome of the studied [4+2] addition, Table 3. Of the 3 possible $Csp^3 - Csp^3$ rotational isomers, only the positive and one of the two negative isomers produce actual free energies of the located TSs not higher than 3 kcal.mol⁻¹ relative to the generally lowest positive NC1, that is, contributing more than 1% to the final product outcome. Contrary to the Curtin-Hammett principle, the TS and product diastereoisomeric distributions are independent of the ground state equilibrium of dienophile conformers due to the large activation free energy of the reaction, some 3 times higher than computed rotational barriers in AS [30]; Table 2 and Fig. 2.

More detailed inspection of Tables 1S and 3 shows nevertheless that some isomeric TSs are higher by less than 1 kcal.mol⁻¹ than NC1pos, Fig. 3, and contribute 5% or more to the final products. These TSs deserve additional attention to their internal interactions for understanding the overall stereoselectivity. However, TSs and their internal interactions are different with various used functionals. We therefore select the numerical models reproducing most closely the known experimental selectivities [22], namely M06L, M06-2x, and MN12sx, in order to interpret TS internal interactions and the origins of selectivity, Table 3 and Fig. 3.

Energies and selected interatomic distances outlined in Fig. 3 for energetically preferred TSs show close contacts of dienophile carbonyl atoms with hydrogen atoms of the diene in the range of 2.3 to 2.5 Å, which can be interpreted as non-classical hydrogen bonds C=O...H–C in some of these [27]. The abundance of heteroatoms in the chiral auxiliary may be expected to provide a significant number of opportunities for the forming of such stabilizing contacts, and energy preferences thereof, for some of the conformationally possible diastereoisomeric reaction paths. This is also the qualitative explanation of the necessity to consider computationally all of the 16 possible reaction paths in order to obtain a correct prediction of the reaction stereochemical outcome. Three of the most stable TSs shown in Fig. 3 actually have short H...O contacts with carbonyl atoms of the attacking dienophile, and another three have no H...O close contacts. Neither of the shown TSs dominates computed free activation energies, and consequently the reported experimental distribution of stereoisomeric products [22, 26], indicating the dominant role of electrostatic interactions with other dienophiles [27] would be oversimplified in the case of AS reaction with CPD. Indeed, going back to Fig. 1 we see, that positive β prefers N1

Table 3. Percentage product distributions for the reaction of AS and cyclopentadiene, CPD, predicted by DFT calculations at the 6-311G(d,p) gaussian basis set level in dichloromethane, together with predicted selectivities. **Pos** and **neg** refer to positive and negative dihedral angles β between adjacent carbonyl groups, see Scheme 2 and Fig. 1. Also shown are M06-2x^d and MN12sx^d results at the 6-311++G(d,p) basis set level. Experimental product distribution: *endo* DS (N1:N2) = 54:46; *endo:exo* = 4.8, dichloromethane [22].

TS	PBE	B97D	M06L	M06-2x	M06-2x ^d	M11L	MN12sx	MN12sx ^d
NC1 pos	7.15	16.93	42.52	48.53	26.62	31.29	33.37	30.80
NC2 pos	1.84	5.94	17.39	9.54	12.40	24.47	10.39	20.38
XC1 pos	7.25	13.04	13.67	14.36	7.35	13.10	34.12	5.84
XC2 pos	1.02	2.91	5.42	3.50	3.79	6.77	2.50	3.51
NT1 pos	0.19	0.79	1.11	1.53	2.24	1.20	1.04	2.82
NT2 pos	0.83	1.06	2.77	6.20	9.72	4.53	3.18	2.85
XT1 pos	0.07	0.18	0.16	0.11	0.14	0.25	0.12	0.40
XT2 pos	0.55	1.13	1.03	0.33	0.69	0.39	0.05	5.41
NC1 neg	13.22	9.67	4.53	1.64	3.93	2.34	1.54	6.36
NC2 neg	50.96	36.99	6.65	9.75	19.95	9.75	9.85	11.64
XC1 neg	3.39	2.44	0.67	0.39	0.49	1.02	0.36	0.64
XC2 neg	8.97	5.66	2.57	1.38	1.29	3.00	1.74	1.29
NT1 neg	2.62	1.62	1.19	1.73	9.61	1.18	1.41	6.05
NT2 neg	0.69	0.19	0.29	0.66	1.03	0.35	0.10	1.31
XT1 neg	0.97	1.01	0.0	0.28	0.35	0.31	0.16	0.60
XT2 neg	0.28	0.45	0.0	0.08	0.41	0.05	0.05	0.11
<i>endo:exo</i>	77.5:22.5	73.2:26.8	76.5:23.5	79.6:20.4	85.5:14.5	74.5:25.5	60.9:39.1	82.2:17.8
	3.44	2.73	3.25	3.90	5.89	2.92	1.56	4.62
N1:N2	29.9:70.1	39.7:60.3	64.5:35.5	67.1:32.9	49.6:50.4	46.3:53.7	61.4:38.6	56.0:44.0

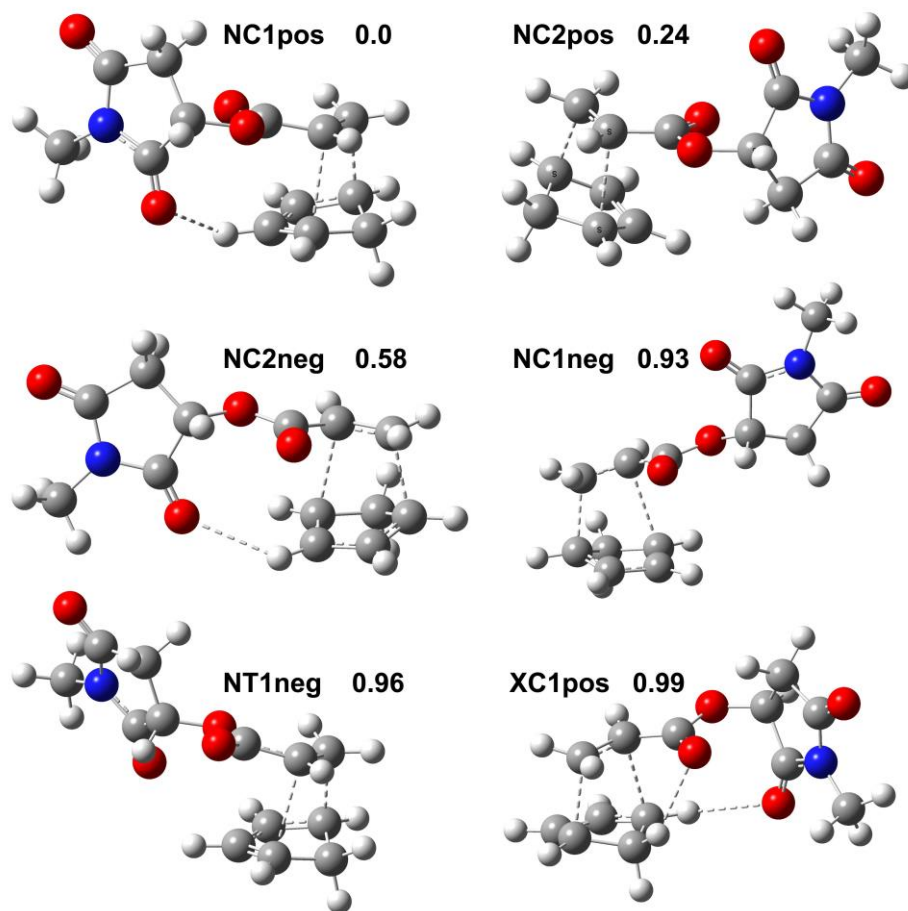


Fig. 3. Energetically preferred transition structures and relative activation free energies at the MN12sx/6-311++G(d,p) level for the [4+2] addition of acryloyl-*S*-hydroxy-*N*-methyl succinimide ASC and cyclopentadiene, CPD, see also Tables 1S and 3. **Pos** and **neg** refer to the respective O=C...C=O dihedral angles β . Short interatomic contacts are outlined as dashed “bonds”: incipient C---C in the range of ca. 2.0 to 2.5 Å; electrostatic contacts C=O...H-C in the range of 2.30 to 2.55 Å.

(*R,R*) selectivity due to the mentioned electrostatic assistance, while negative β prefers N2 (*S,S*) selectivity for the same electrostatic reason. Fig. 3 also shows the 4 most stable *endo* TSs contributing to more than 80% of the predicted population of *endo* TSs. Electrostatic preference to N1 (*R,R*) gives 37%, and to N2 (*S,S*) 32% of the computed total stereochemical outcome, Table 3, which coincides with the observed N1:N2 ratio [22]. It can be seen that in each pair of NC1-NC2 the TSs showing nontraditional hydrogen bonds are more stable than their counterparts. The two diastereoface preferences balance each other to produce the observed low N1:N2 ratio and also contribute to more than 80% of the observed *endo* selectivity. Following in stability are *s-trans* and *exo* TSs, where preferences involve other types of intramolecular interactions along with the electrostatics discussed above, to further complicate


the final experimental stereochemical result. However, as we discuss selectivity changes with the same diene, and *s-cis/s-trans* isomers of the same dienophile, no changes of frontier orbital, or secondary orbital effects, anomeric effects, substituent electronegativity or hyperconjugative aromaticity/antiaromaticity may partake in the present case [31, 32].

CONCLUSION

The reported results show a success of extensively parameterized high-performance functionals as M06L, M06-2x, and MN12sx in the reproduction of observed low diastereoselectivity of the title DA reaction. We find that the full palette of intramolecular interactions, rather than non-traditional H bonds only, govern the diastereofacial

selectivity of the AS + CPD addition, as further substantiated by diffuse basis set M062x/6-311++G(d,p) and MN12sx/6-311++G(d,p) TS optimizations.

Acknowledgements: A part of the reported computations has been carried out on the MADARA HPC cluster, IOCCP, acquired under Project RNF01/0110 (2009-2011) of the National Research Fund of Bulgaria.

Electronic Supplementary Data available here 

REFERENCES

1. O. Diels, K. Alder, *J. Liebig's Ann. Chem.*, **460**, 98 (1928).
2. R. B. Woodward, R. Hoffmann, *Angew. Chem. Int. Ed.*, **8**, 781 (1969).
3. R. Hoffmann, R. B. Woodward, *Science*, **167** (3919), 825 (1970).
4. M. J. S. Dewar, S. Olivella, J. J. P. Stewart, *J. Am. Chem. Soc.*, **108**, 5771 (1986).
5. K. N. Houk, Y. T. Lin, F. K. Brown, *J. Am. Chem. Soc.*, **108**, 554 (1986).
6. E. Goldstein, B. Beno, K. N. Houk, *J. Am. Chem. Soc.*, **118**, 6036 (1996).
7. W. Koch, M. C. Holthausen, *A Chemist's Guide to Density Functional Theory*, 2nd edition, Wiley-VCH, 2001.
8. S. N. Pieniazek, F. R. Clemente, K. N. Houk, *Angew. Chem. Int. Ed.*, **47**, 7746 (2008).
9. Y. Zhao, D. G. Truhlar, *Theor. Chem. Acc.*, **120**, 215 (2008).
10. Y. Zhao, D. G. Truhlar, *Acc. Chem. Res.*, **41**, 157 (2008).
11. Y. Zhao, D. G. Truhlar, *J. Chem. Theory Comput.*, **7**, 669 (2011).
12. W. J. Hehre, L. Radom, P. v. R. Schleyer, J. A. Pople, *Ab Initio MO Theory*, Wiley, NY, 1986.
13. Gaussian 09, Revision D.01: M. J. Frisch, G. W. Trucks, H. B. Schlegel, G. E. Scuseria, M. A. Robb, J. R. Cheeseman, G. Scalmani, V. Barone, B. Mennucci, G. A. Petersson, H. Nakatsuji, M. Caricato, X. Li, H. P. Hratchian, A. F. Izmaylov, J. Bloino, G. Zheng, J. L. Sonnenberg, M. Hada, M. Ehara, K. Toyota, R. Fukuda, J. Hasegawa, M. Ishida, T. Nakajima, Y. Honda, O. Kitao, H. Nakai, T. Vreven, J. A. Montgomery, Jr., J. E. Peralta, F. Ogliaro, M. Bearpark, J. J. Heyd, E. Brothers, K. N. Kudin, V. N. Staroverov, T. Keith, R. Kobayashi, J. Normand, K. Raghavachari, A. Rendell, J. C. Burant, S. S. Iyengar, J. Tomasi, M. Cossi, N. Rega, J. M. Millam, M. Klene, J. E. Knox, J. B. Cross, V. Bakken, C. Adamo, J. Jaramillo, R. Gomperts, R. E. Stratmann, O. Yazyev, A. J. Austin, R. Cammi, C. Pomelli, J. W. Ochterski, R. L. Martin, K. Morokuma, V. G. Zakrzewski, G. A. Voth, P. Salvador, J. J. Dannenberg, S. Dapprich, A. D. Daniels, O. Farkas, J. B. Foresman, J. V. Ortiz, J. Cioslowski, D. J. Fox, Gaussian, Inc., Wallingford CT, 2013.
14. J. P. Perdew, K. Burke, M. Ernzerhof, *Phys. Rev. Lett.*, **77**, 3865 (1996).
15. J. P. Perdew, K. Burke, M. Ernzerhof, *Phys. Rev. Lett.*, **78**, 1396 (1997).
16. S. Grimme, *J. Comp. Chem.*, **27**, 1787 (2006).
17. R. Peverati, D. G. Truhlar, *J. Phys. Chem. Lett.*, **2**, 2810 (2011).
18. R. Peverati, D. G. Truhlar, *J. Phys. Chem. Lett.*, **3**, 117 (2012).
19. R. Peverati, D. G. Truhlar, *J. Chem. Theory and Comput.*, **8**, 2310 (2012).
20. S. S. Shaik, H. B. Schlegel, S. Wolfe, *Theoretical aspects of physical organic chemistry*, Wiley, 1992. H. B. Schlegel, *J. Comp. Chem.* **3**, 214 (1982).
21. J. Tomasi, B. Mennucci, R. Cammi, *Chem. Rev.*, **105**, 2999 (2005).
22. T. Poll, *Neue chirale Auxiliare für die asymmetrische Diels-Alder-Reaktion*, PhD Thesis., Univ. Würzburg, 1988, pp. 133–134; 143–146.
23. M. S. Betson, J. Clayden, H. K. Lam, M. Helliwell, *Angew. Chem. Int. Ed. Engl.*, **44**, 1241 (2005).
24. K. Kahn, T. C. Bruice, *Bioorg. Med. Chem.*, **8**, 1881 (2000).
25. T. H. Lowry, K. S. Richardson, *Mechanism and Theory in Organic Chemistry*, 3rd Edition, Harper International, 1987, pp. 202–229.
26. T. Poll, G. Helmchen, B. Bauer, *Tetrahedron Lett.*, 2191 (1984).
27. S. M. Bakalova, A. G. Santos, *J. Org. Chem.*, **69**, 8475 (2004).
28. W. J. Hehre, R. Ditchfield, J. A. Pople, *J. Chem. Phys.*, **56**, 2257 (1972).
29. T. Clark, J. Chandrasekhar, P. v. R. Schleyer, *J. Comp. Chem.*, **4**, 294 (1983).
30. I. G. Pojarlieff, *Physical Organic Chemistry and Dynamic Stereochemistry* (in Bulgarian), Sofia, 2001, pp. 65–70.
31. B. J. Levandowski, Z. Lufeng, K. N. Houk, *J. Comput. Chem.*, **37**, 117 (2016).
32. B. J. Lewandowski, K. N. Houk, *J. Am. Chem. Soc.*, **138**, 16731 (2016).

СТЕРЕОСЕЛЕКТИВНОСТ НА ДИЛС–АЛДЕРОВОТО ПРИСЪЕДИНЯВАНЕ НА [S]-АКРИЛОИЛ-N-МЕТИЛ СУКЦИНИМИД И ЦИКЛОПЕНТАДИЕН: ПРОИЗХОД И ИЗЧИСЛИТЕЛНО МОДЕЛИРАНЕ В РАМКИТЕ НА ТЕОРИЯТА НА ФУНКЦИОНАЛА НА ПЛЪТНОСТТА

С. М. Бакалова, Х. Канети

¹ *Институт по Органична Химия с Център по Фитохимия, Българска Академия на Науките, ул. Акад. Г. Бончев, бл. 9, 1113 София, България*

Постъпила на 02 март 2017 г.; Коригирана на 24 март 2017 г.

(Резюме)

Изследвана е реакция на Дилс–Алдер с ниска диастереоселективност за сравнение на изчислителните предвиждания от теорията на функционала на плътността с различни нива на параметризация. Показано е, че експерименталната диастереоселективност от 55:45, която отговаря кинетично на разлики между свободните енергии на активация по-малки от 1 ккал.мол⁻¹, може да бъде възпроизведена задоволително от пресмятания с помощта на подобрените по точност функционали M06L, M06-2x и MN12sx в случай, че са подходящо отчетени конформационните разпределения на реагентите. В конкретния изследван случай това е диенофилът *S*-хидрокси-*N*-метилсукцинимид акрилат. Изчислено е, че важните приноси на вътрешно-молекулните и междумолекулните взаимодействия към намерените диастереомерни преходни структури не се дължат предимно на електростатични взаимодействия. Участието на дисперсионни и по-далечни сили в *ендо:екзо* селективността е отчетено от по-новите параметри в пресмятанията.